IMPROVEMENT AND SENSITIVITY ANALYSIS OF EQUIVALENT HEAT TRANSFER MODEL FOR DYNAMIC THERMAL RATING OF OVERHEAD LINES

by

Xiangyang PENG [a], ***Honglei DENG*** [b], ***Rui WANG*** [a], ***Zhao LIU*** [b], ***Shujian LUO*** [a], ***Deming GUO*** [b*], ***and Gang LIU*** [b*]

[a] Guangdong Key Laboratory of Electric Power Equipment Reliability, Electric Power Research Institute of Guangdong Power Grid Co., Ltd., Guangzhou, China
[b] School of Electric Power Engineering, South China University of Technology, Guangzhou, China

Original scientific paper
https://doi.org/10.2298/TSCI210611020P

With the rapid growth of power demand, the conductor ampacity calculation method based on the dynamic thermal rating (DTR) becomes more and more important. Based on the shortcomings of the current DTR models, a new DTR model that does not need to measure the wind speed and the operating state of conductor is proposed, which is called the equivalent heat transfer (EHT) model. However, there are still shortcomings in the accuracy of the EHT model in application. In this paper, the EHT model is improved at first according to the consideration of the effect of air physical parameters and the redetermination of the experimental parameters of the EHT equipment. Then, the operation of EHT equipment is simulated through the established experimental platform. The improved EHT model is verified by the IEEE standard. Finally, the sensitivity analysis of the improved EHT model is carried out. The results show that the improved EHT model is greatly improved on application accuracy compared to the original EHT model. Moreover, the improved EHT model can choose the steady-state temperature at any position on the surface of the aluminum ball to calculate the conductor ampacity, and the relative error does not exceed 6%. The improved EHT model is reliable and can meet the safe operation requirements of the power system in practical engineering applications.

Key words: *conductor ampacity, improved EHT model, sensitivity analysis, overhead lines, and heat transfer*

Introduction

With the rapid economic development, the demand for electricity continues to increase. However, limited by the challenges such as long construction period, difficult land acquisition, ecological and environmental protection requirements, *etc.*, it is difficult in investment and construction of new overhead lines to meet the urgent demand of electricity for economic development [1, 2]. As a result, taking full advantage of the transmission capacity of existing overhead lines can alleviate this urgent demand [3, 4].

The transmission capacity of the overhead lines can be characterized by the ampacity. The ampacity refers to the maximum current that meets the design safety standards of the overhead lines, while the conductor is at the maximum allowable operating temperature [5]. At present, the static thermal rating (STR) technology has been widely used, while the calculated

[*] Corresponding author, e-mails: 201720113678@mail.scut.edu.cn, liugang@scut.edu.cn

conductor ampacity is generally conservative [6]. Practically, the heat dissipation conditions of overhead lines in the actual operating environment are far better than the hypothetical conditions of STR. Therefore, a DTR technology has been proposed [7]. The DTR technology is to calculate the actual conductor ampacity according to the real-time weather conditions and conductor operating conditions [8-10]. It can give full play to the power transmission capacity of the conductors [9, 10].

In recent years, many DTR models have been developed [11]. For example, models based on weather parameters need to measure the weather parameters such as ambient temperature, solar irradiance, and wind speed [12]. However, many sensors have to be involved. Especially, for wind speed sensors, there are problems such as large measurement errors and expensive cost [13]. The model based on the operating state of the conductors needs to measure the temperature and sag of the conductors [14, 15]. For this type of DTR model, the sensor requires to be installed or serviced after power outage, which makes daily operation and maintenance difficult [16].

Liu *et al*. [17] proposed a DTR model that did not need to measure the wind speed or the operating state of the conductors, which was called the EHT model. The model indirectly reflected the convective heat loss rate of the conductors by monitoring the steady-state thermal behavior of an ideal aluminum, Al, ball, so as to realize the evaluation of the conductor ampacity. Since the convective heat loss rate changes in real time, the steady-state thermal behavior of Al ball is also variable in real time. In this situation, the calculated conductor ampacity changes in real-time. The verification of the model was finished based on finite element modelling. In this case, the thermal behavior of the ideal Al ball can be obtained by the finite element method. However, in practical applications, there are structural differences between the Al ball in the EHT model and the ideal Al ball. At present, the calculation error caused by this structural difference is not clear. In addition, in the process of establishing the relationship between the Al ball and the conductor, the influence of the air physical parameters is also not considered.

In this paper, the EHT model is improved firstly. On the one hand, the correlation between the conductor and the Al ball is reestablished through theoretical analysis. The influence of the air physical parameters is emphatically considered. On the other hand, according to the theoretical calculation formula of the Al ball convection heat transfer, the experimental parameters of the Al ball of the EHT equipment are calculated. Then, the operation of the EHT equipment (including the Al ball) in application is simulated through the wind tunnel experiment platform. By comparing with the calculation results of the conductor ampacity in the IEEE standard, the improvement effect of the EHT model is analyzed, and the accuracy of the improved EHT model is verified. Finally, the sensitivity analysis of the improved EHT model is presented, and the critical condition of model reliability is determined.

The equivalent heat transfer model

Calculation process of the equivalent heat transfer model

The EHT model is a model that realizes the DTR calculation of the overhead lines based on the correlation of heat loss between the heating Al ball and the conductors in the same environment. This model involves a heating Al ball, which is placed near the overhead conductor. Since the Al ball and the conductor are in the same environment, their weather conditions (including ambient temperature, solar irradiance, and wind) are the same. Based on this situation, the heat loss of the Al ball can be calculated by the thermal behavior of the Al ball (*i.e.*, steady-state temperature) in a certain environment. According to the correlation of the heat loss between the Al ball and the conductor, the convective heat loss of conductor is obtained. Then the ampacity of conductor in this environment can be evaluated. As a result, the Al ball is used to indirectly calculate the convective heat loss of conductor.

The steady-state thermal behavior of the Al ball can be expressed by the heat balance equation:

$$q_{\mathrm{cs}} + q_{\mathrm{rs}} = q_{\mathrm{ss}} + q_{\mathrm{gs}} \tag{1}$$

where q_{cs}, q_{rs}, q_{ss}, and q_{gs}, respectively, are the convective heat loss rate, the radiant heat loss rate, the solar heat gain rate, and the internal heat source rate of the Al ball. The solar heat gain rate q_{ss} and the radiant heat loss rate q_{rs} of the Al ball can be easily calculated according to the monitored weather parameters [17].

After setting the heat source power in the Al ball (*i.e.* q_{gs}), the steady-state temperature results of the Al ball can be used to calculate its convective heat loss rate q_{cs}. Through the Newton cooling formula, the convective heat transfer coefficient of the Al ball can be obtained:

$$h = \frac{q_{\mathrm{cs}}}{\pi l^2 (T_{\mathrm{s}} - T_{\mathrm{a}})} \tag{2}$$

where h is the convective heat transfer coefficient of the Al ball, l and T_{s} are the diameter and surface temperature of the Al ball, respectively, and T_{a} is the ambient temperature.

In the heat transfer theory, the convective heat transfer coefficient is related to a series of dimensionless parameters. The convection heat transfer includes two forms: natural-convection and forced convection. The natural-convection can be equivalent to the forced convection with wind speed not exceeding 0.2 m/s [17, 18]. Therefore, the convective heat transfer of the Al ball can be treated in the form of forced convection. That is, the relationship between the convective heat transfer coefficient of the Al ball and the related dimensionless parameters can be written [19]:

$$\mathrm{Nu} = \frac{hk_{\mathrm{s}}}{l} \tag{3}$$

$$\mathrm{Nu} = 2 + \left(a\mathrm{Re}_{\mathrm{s}}^{1/2} + b\mathrm{Re}_{\mathrm{s}}^{2/3}\right)\mathrm{Pr}^{0.4}\left(\frac{\mu_{\mathrm{s}}}{\mu_{\mathrm{w}}}\right)^{1/4} \tag{4}$$

where k_{s} is the thermal conductivity of air, μ_{s} and μ_{w} are the dynamic viscosity of air at the characteristic temperature and the average surface temperature of the Al ball, respectively, a and b are constant parameters. The Re_{s}, Pr, and Nu are all dimensionless parameters, which are the Reynolds number, Prandtl number, and Nusselt number of the Al ball, respectively. Whitaker [19] provides the parameters (*i.e.*, k_s, μ_s, μ_w, Pr, a and b) in eqs. (3) and (4), where $a = 0.4$, $b = 0.06$ in [19].

The correlation of Reynolds numbers between the conductor and the Al ball [17]:

$$\mathrm{Re}_{\mathrm{c}} = \frac{D_0}{l}\mathrm{Re}_{\mathrm{s}} \tag{5}$$

where Re_{c} is the Reynolds number of the conductor and D_0 is the diameter of the conductor. Therefore, after determining the convective heat transfer coefficient of the Al ball, the Reynolds number, Re_{s}, of Al ball can be obtained according to eqs. (3) and (4). Furthermore, the Reynolds number, Re_{c}, of the conductor can be calculated based on eq. (5).

Similarly, the steady-state heat balance equation of the conductor is shown:

$$I^2 R(T_{\mathrm{c}}) + q_{\mathrm{s}} = q_{\mathrm{r}} + q_{\mathrm{c}} \tag{6}$$

where q_s, q_c, q_r, are the solar heat gain rate, the convective heat loss rate, and the radiant heat loss rate per unit length of the conductor, respectively, I is the AC current of conductor, and $R(T_c)$ is the AC resistance of the conductor per unit length when the conductor temperature is T_c. When the conductor temperature T_c takes the maximum allowable operating temperature $T_{c,max}$ (70 °C), the calculated current value is the ampacity I_{amp} of the conductor:

$$I_{amp} = \sqrt{\frac{q_c + q_r - q_s}{R(T_{c,max})}} \tag{7}$$

The solar heat gain rate q_s and radiant heat loss rate q_r of the conductor can be easily determined by weather parameters, and the convective heat loss rate q_c is determined by the equations related to the conductor Reynolds number, Re_c. The expressions of the aforementioned parameters, including $R(T_c)$, q_s, q_c, q_r, *etc.*, can be found in the IEEE standard [18].

Combining with the flowchart of calculating the conductor ampacity in the EHT model in fig. 1, this model can avoid the shortcomings of inaccurate calculation of the conductor ampacity caused by the measurement error of the wind speed sensor. In this paper, the type of conductor is ACSR 240/30 mm^2 for the ampacity calculation.

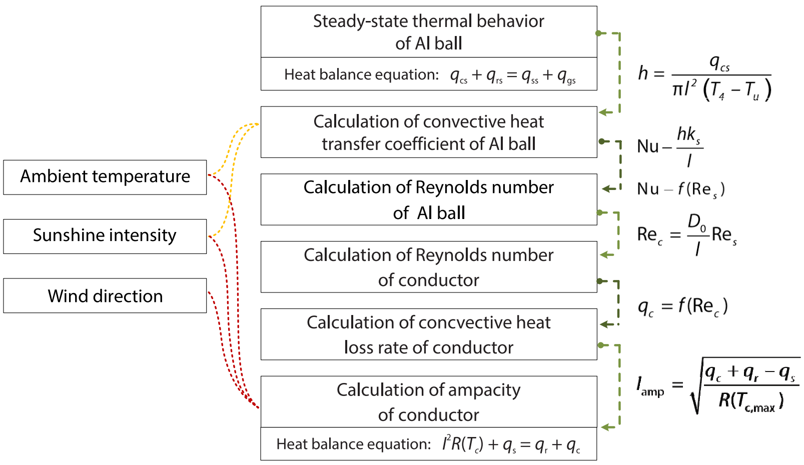

Figure 1. Calculation flowchart of conductor ampacity in the EHT model

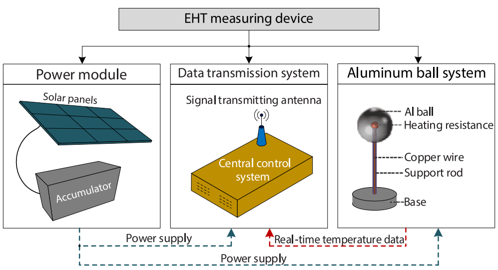

Figure 2. Schematic diagram of the EHT equipment

The equivalent heat transfer equipment

The basic composition of the EHT equipment includes a power module, a data transmission system, and an Al ball system, as shown in fig. 2.

The solar energy system is used as the power module. The data transmission system consists of a signal transmitting antenna and a central control system, and the TCP protocol is used to transmit data. For the Al ball system, a heating resistor is placed in the center of the Al ball, and the heating resistor and the power supply are connected by copper wires. The Al ball needs to be supported and fixed, so a support rod made of polyether ether ketone matrix composite with good thermal insulation performance is designed at the bottom of the Al ball [20].

Improvement of the equivalent heat transfer model

In the EHT model, the physical parameters such as the air density and the air dynamic viscosity are ignored in the process of establishing the correlation of the Reynolds numbers between the conductor and the Al ball. Moreover, the determined experimental correlation parameters in the Al ball convection heat transfer are derived based on the ideal Al ball. However, the Al ball in the actual EHT equipment is different from the ideal Al ball. Therefore, it is necessary to improve the existing EHT model to reduce or eliminate the errors caused by the previous two points.

Improvement of correlation between the conductor and the Al ball

According to the Reynolds number eqs. (8) and (9) of the conductor and the Al ball, the relational expression of the Reynolds numbers between the conductor and the Al ball is as shown:

$$\mathrm{Re}_\mathrm{c} = \frac{D_0 \rho_\mathrm{f} V_\mathrm{w}}{\mu_\mathrm{f}} \tag{8}$$

$$\mathrm{Re}_\mathrm{s} = \frac{l \rho_\mathrm{s} V_\mathrm{w}}{\mu_\mathrm{s}} \tag{9}$$

$$\mathrm{Re}_\mathrm{c} = \frac{\rho_\mathrm{s}\mu_\mathrm{f}}{\rho_\mathrm{f}\mu_\mathrm{s}} \frac{D_0}{l} \mathrm{Re}_\mathrm{s} \tag{10}$$

where ρ_s and ρ_f, represent the air density at the characteristic temperature of the Al ball and the conductor, respectively, μ_s and μ_f, represent the air dynamic viscosity at the characteristic temperature of the Al ball and the conductor, respectively. The characteristic temperature of the Al ball is equal to the ambient temperature T_a. The characteristic temperature of the conductor is equal to the average value of the conductor temperature and the ambient temperature [18]:

$$\mathrm{g}(T_\mathrm{a}) = \frac{\rho_\mathrm{s}\mu_\mathrm{f}}{\rho_\mathrm{f}\mu_\mathrm{s}} = \frac{\rho(T_\mathrm{a})\mu\left(\dfrac{T_\mathrm{a}+70}{2}\right)}{\rho\left(\dfrac{T_\mathrm{a}+70}{2}\right)\mu(T_\mathrm{a})} \tag{11}$$

Let eq. (11) as a correction function of the correlation eq. (5) between the Al ball and the conductor. It is a function related only to the ambient temperature. Compared with the correlation eq. (5), the correlation eq. (10) improved by the correction function considers the differences for the air density and air dynamic viscosity of the Al ball and the conductor. The improved model can get a more accurate calculation result of conductor ampacity.

Improvement of experimental correlation parameters in convection heat transfer of the Al ball

Through the introduction of the EHT equipment in section *The equivalent heat transfer equipment*, it is found that the Al ball in the EHT equipment is connected by a support rod. This is the structure difference from the ideal Al ball. The heat insulation of the support rod is not absolute (0.25 W/mK). The influence of the support rod on the thermal behavior of the Al ball is analyzed by the finite element modelling.

According to the structure of the EHT equipment, a finite element simulation model of the Al ball system is established by using the finite element software COMSOL. The radius of the Al ball is 1.5 cm. There is a cylindrical heating space with a radius of 0.3 cm and a height of 0.5 cm in the center of the Al ball. The size of this cylindrical heating space is the same as that of heating resistor. The heating resistor is connected to the power supply through two copper wires, and the heat source power is 0.75 W. In addition, the length of the support rod is 15 cm. The boundary conditions of the thermal field contain the heat radiation and heat convection on the surface of Al ball. The simulation of heat radiation is achieved by setting the emissivity of the Al. In this section, the emissivity is set as 0.2 for calculation. The simulation of heat convection is realized by thermal-fluid coupling. Then, the standard k-ε model of the turbulence model is adopted to solve the fluid field. Moreover, it is noted that the effect of air gravity is also considered during the solution of fluid field.

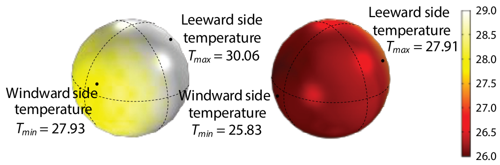

Figure 3. Thermal behavior of ideal Al ball and Al ball with support rod

Figure 3 shows the steady-state temperature distributions of the ideal Al ball and the Al ball with a support rod with the ambient temperature of 20 °C and a wind speed of 1 m/s. On the left side of the picture is the ideal Al ball, and on the right side of the picture is the Al ball with a support rod. From the figure, the temperature of the Al ball with the support rod is lower than that of the ideal Al ball overall. Therefore, the support rod can affect the thermal behavior of the Al ball.

In the EHT model, the parameters a and b in the convection heat transfer of the Al ball as shown in eq. (4) are determined by the experimental correlation formula [17, 19]. First, based on the heat balance eq. (1), the thermal behavior of the Al ball under different environmental conditions is obtained through experiments. Combining the Al ball temperature with the weather data obtained from the measurement, the Nusselt number of the Al ball can be derived from eqs. (1)-(3). On the other hand, according to the calculation eq. (9), the Al ball Reynolds number under the corresponding conditions can be obtained. Defining the parameter Y according to eq. (12), and based on eqs. (4) and eq. (12), eq. (13) can be derived, which shows a set of data points of Y and Reynolds number that are related to each other. The least square method can be used to solve the parameters a and b in the equation. When the experimental object is an ideal ball, the parameters a and b are determined to be 0.4 and 0.06 [19]:

$$Y = \frac{\mathrm{Nu}-2}{\mathrm{Pr}^{0.4}\left(\dfrac{\mu_\mathrm{s}}{\mu_\mathrm{w}}\right)^{1/4}} \tag{12}$$

$$Y = a\mathrm{Re}_\mathrm{s}^{1/2} + b\mathrm{Re}_\mathrm{s}^{2/3} \tag{13}$$

There is a structural difference between the Al ball of the EHT equipment and the ideal ball. In other words, the research object of this paper is the Al ball with a supporting structure. Therefore, the parameters a and b obtained by the ideal ball are not suitable for the actual model. It is necessary to re-determine the values of parameters a and b for the Al ball of the EHT equipment in practical applications. Firstly, the temperature distribution of the Al ball under the operating conditions is obtained through finite element simulation, in which, the ambient temperature is in the range of 0-40 °C, and the wind speed is in the range of 0-10 m/s.

In this section, the calculation result of the minimum surface temperature of the Al ball is used for the fitting analysis. According to the method of determining the parameters a and b in the EHT model, the data correlation between Y including Nusselt number and Reynolds number is obtained by eqs. (1)-(4) and eq. (12), as shown in fig. 4. It is found intuitively from the figure that there is a linear relationship between Y and Reynolds number in logarithmic co-ordinates. According to the principle of the least square method and combining with MATLAB to fit this set of data, the parameters a and b are 0.6401 and 0.1534, respectively.

To test the adaptability of the obtained parameters and ensure the effectiveness and practical applicability of the curve fitting, it is necessary to carry out residual analysis on the fitting results. The R^2 is introduced to reflect the fitting degree of the curve, and the result is 0.9966, which is close to 1. This shows that the fitting is good and the reliability is high [21].

To sum up, based on the improvement of the correlation between the Al ball and the conductor by the correction function, and based on the improvement of the experimental correlation parameters in the convection heat transfer of Al ball, an improved EHT model is obtained.

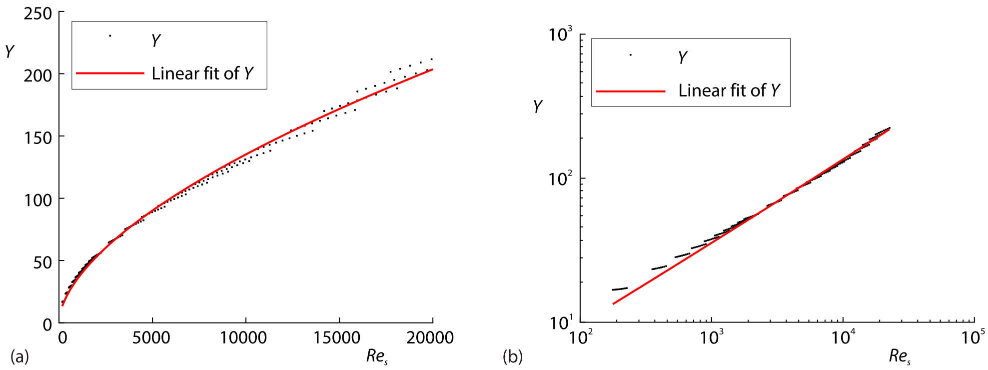

Figure 4. Correlation between Nusselt number and Reynolds number; (a) linear co-ordinate and (b) logarithmic co-ordinates

Experimental verification

Experimental system and scheme

For the purpose to verify the accuracy of the improved EHT model in practical application and the improvement effect of the model, a wind tunnel experimental platform is designed and built to simulate various weather conditions. The schematic diagram of the wind tunnel experimental platform is shown in fig. 5.

The entire experimental system is divided into two parts: the Al ball temperature rise measurement system and the wind tunnel experimental system. The Al ball temperature rise measurement system includes a DC stabilized power supply, a temperature recorder, thermocouples, and an Al ball system. The DC stabilized power supply can adjust the power of the heating resistor. The temperature measurement range of the thermocouples is –200~350 °C, and its error is ±0.5 °C. Thermocouples are, respectively placed on the windward side, leeward side, and crosswind side of Al ball (*i.e.*, points of T_1, T_2, and T_3 in fig. 6) to measure the temperature distribution of the Al ball.

The wind tunnel experiment system is a fully enclosed circulation system, which can make the air-flow of the operating platform stable, and the wind speed tends to be sta-

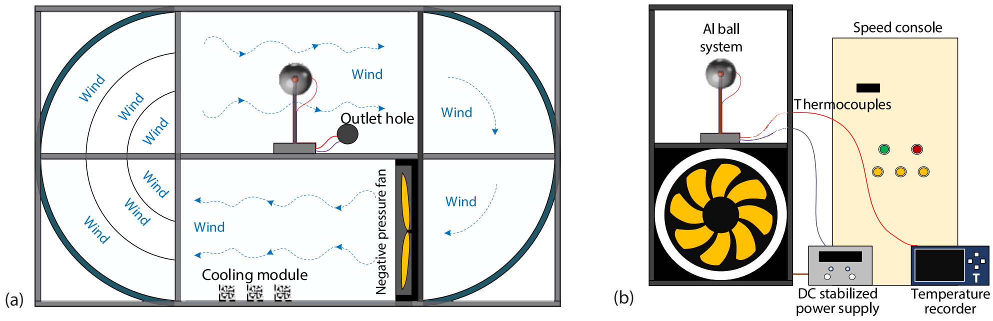

Figure 5. Schematic diagram of wind tunnel experimental platform; (a) side view and (b) front view

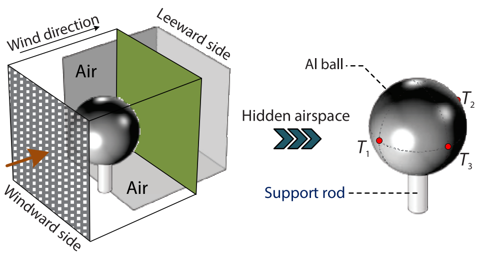

Figure 6. Schematic diagram of thermocouple lay-out for measuring surface temperature of Al ball

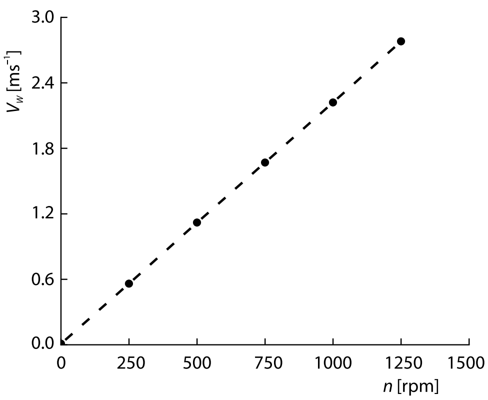

Figure 7. Correlation between wind speed and motor speed

bilized [22]. The dimension of the operating platform is 1250 mm × 1100 mm × 900 mm, which is enough to ensure that the temperature field around the Al ball is not affected by the wind tunnel wall. The wind tunnel experiment system includes two parts: a wind speed control system and a temperature control system. The wind speed control system is composed of a negative pressure fan and a speed console. The speed console controls the speed of the negative pressure fan through a servo motor to adjust the wind speed. A thermosensitive anemometer is used to measure the wind speed during the experiment with the range of 0.2-10 m/s, the resolution of 0.01 m/s, and the error of ±0.1 m/s. The rotate speed of the motor (*i.e.*, n in fig. 7) has a linear correlation with the measured wind speed (*i.e.*, V_w in fig. 7), as shown in fig. 7. The temperature control system consists of an air conditioner and a cooling module. The air conditioner can adjust the temperature range of the experiment environment. The power of the cooling module is 0~600 W, which is used to discharge the heat generated by the motor out of the operating platform.

To achieve the verification of the improved EHT model, the thermal behavior of the Al ball should be obtained. Therefore, the following experimental scheme is set up in this paper. A constant heat source power of 0.75 W is applied to the Al ball within the range of ambient temperature of 20-34 °C. The steady-state experiment of the Al ball equipment at the rotate speed n of 250 rpm, 500 rpm, 750 rpm, and 1000 rpm are conducted, respectively, and the steady-state temperature at the windward side, leeward side, and crosswind side of Al ball are recorded.

Discussion of experimental results

The thermal behavior of the Al ball is obtained by the wind tunnel experiment platform. The recorded Al ball temperature and the corresponding wind speed and ambient temperature are brought into the original EHT model to calculate the ampacity of conductor, and the ampacity is compared with the ampacity calculated by the IEEE standard under the same meteorological conditions. The result is shown in fig. 8. The black dots (▼) represent the ampacity result I_{str} calculated by the IEEE standard. The red (●), blue (▲), and green (■) points, respectively represent the ampacity results calculated from the windward side temperature, leeward side temperature, and crosswind side temperature of Al ball, respectively.

In fig. 8, no matter whether the temperature calculation on the windward, leeward or crosswind sides of the Al ball is selected, the calculated ampacity curves are all above the IEEE standard. In other words, the ampacity calculated by using the EHT model at any point on the surface of the Al ball is greater than that calculated by the IEEE standard. This is because the heat loss of the Al ball is not only composed of the radiation heat loss and convection heat loss, but also part of the heat is lost to the support rod through heat conduction. This leads to a decrease in the overall temperature of the Al ball. Therefore, the heat loss of the current environment is overestimated, and then a higher ampacity value is calculated.

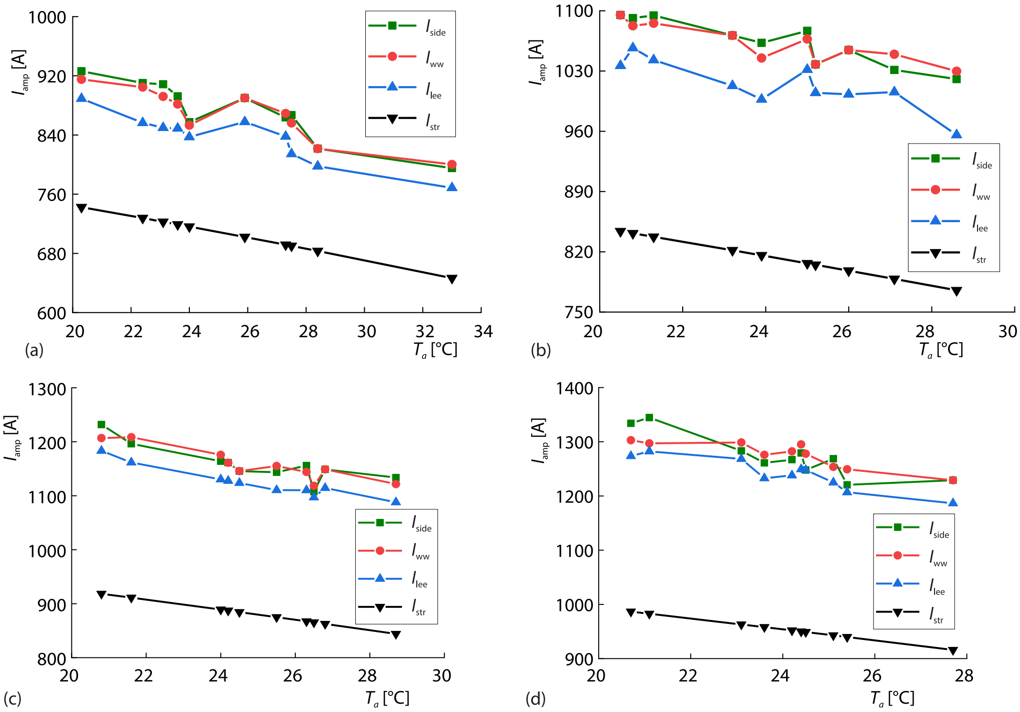

Figure 8. Comparison of ampacity results from original EHT model and IEEE standard; (a) V_w = 0.56 m/s, (b) V_w = 1.12 m/s, (c) V_w = 1.67 m/s, and (d) V_w = 2.22 m/s

Figure 9 shows the relative error between the ampacity results of the original EHT model and the IEEE standard in the form of a bar graph. In the figure, the red – 2, blue – 3, and green – 1 bar graphs, respectively represent the relative errors between the ampacity results calculated from the windward side temperature, leeward side temperature, and crosswind side temperature of the Al ball. They are represented by err_{ww}, err_{lee}, and err_{side}, respectively and calculated by eq. (14). With the increase of wind speed, the error shows an upward trend. The ampacity error calculated from the temperature on the leeward side of the Al ball is less than that on the windward and crosswind sides. However, in all the results calculated by the original EHT model, the minimum relative error is more than 16% and the maximum is 37%. Therefore, excessive conductor ampacity results can lead to the incorrect assessments in engineering. In this situation, the conductor may overheat. This is unacceptable to the power system:

$$err_x = \frac{|I_x - I_{str}|}{I_{str}} \times 100\%, \ (x = \text{ww}, \text{lee}, \text{side}) \tag{14}$$

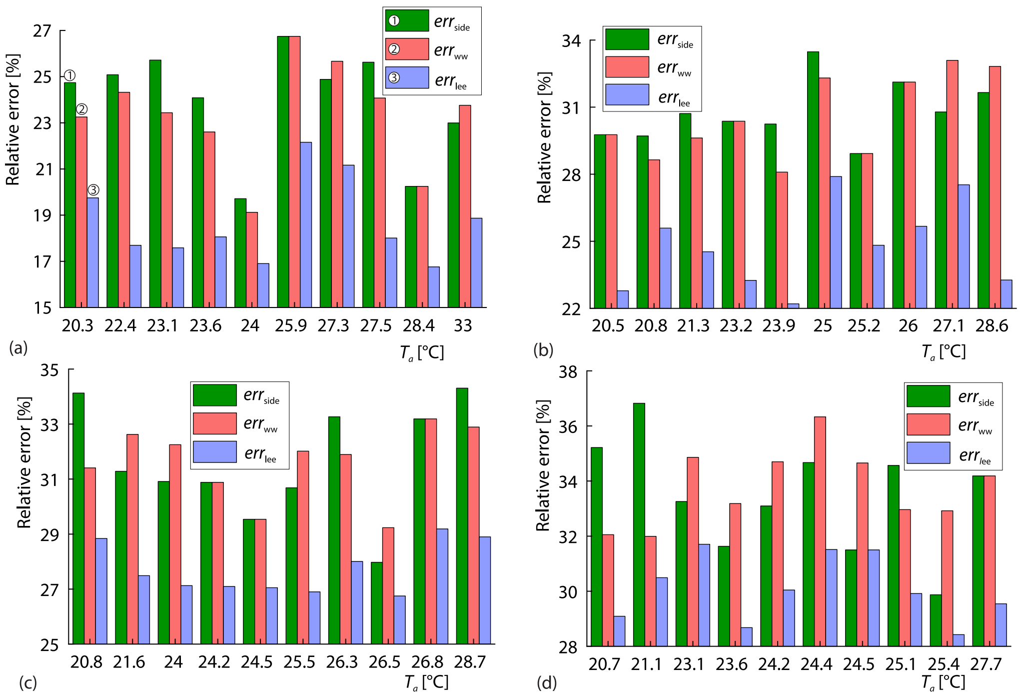

Figure 9. Relative errors of ampacity results from original EHT model and IEEE standard; (a) V_w = 0.56 m/s, (b) V_w = 1.12 m/s, (c) V_w = 1.67 m/s, and (d) V_w = 2.22 m/s

Then, the experimental data is brought into the improved EHT model to calculate the conductor ampacity, the IEEE standard calculation is conducted under the same meteorological conditions, and the relative errors are also calculated. The results are shown in figs. 10 and 11.

In fig. 10, the ampacity results calculated by the improved EHT model decrease with the increase of ambient temperature and increase with the increase of wind speed. The ampacity calculated from the temperature measured at any position on the surface of the Al ball is basically below the calculation result of the IEEE standard. In other words, the conductor ampacity results calculated by the improved EHT model are all lower than that of the IEEE standard calculation results.

In fig. 11, the maximum error of ampacity calculated by the leeward side temperature is no more than 6%, while the ampacity errors calculated from the windward and crosswind sides temperature of the aluminum ball are relatively small, and the maximum is not more than 5%. This is because the improved EHT model is obtained through the experimental correlation formula, *i.e.*, eq. (4), based on the finite element simulation data on the windward side of the Al ball. In addition, the temperatures on the windward and crosswind sides measured during the experiment are relatively close.

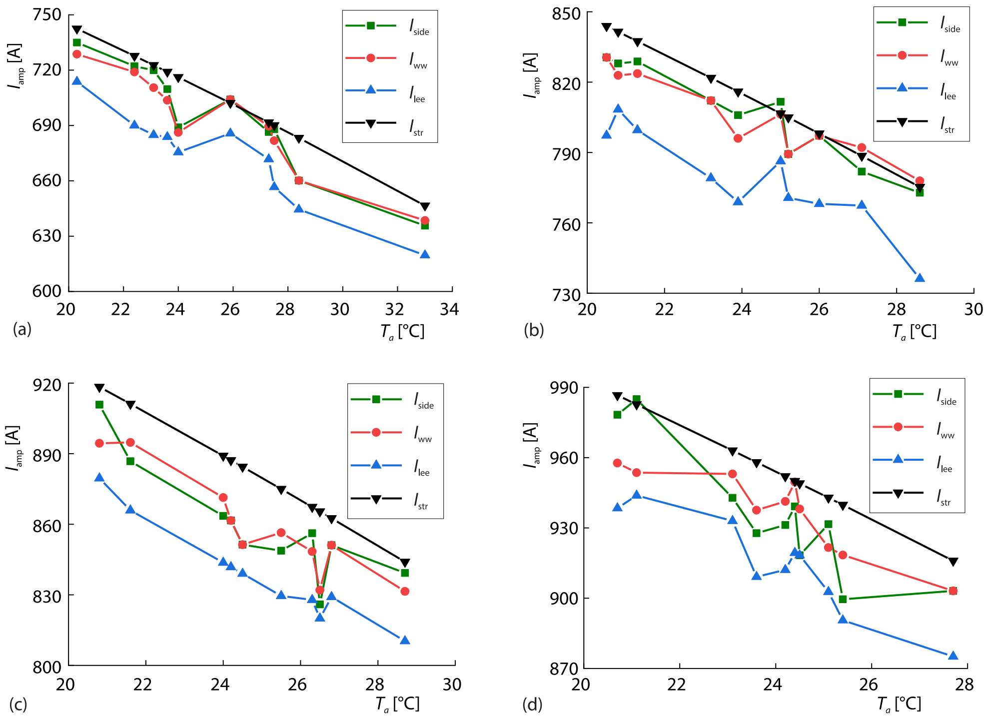

Figure 10. Comparison of ampacity results from improved EHT model and IEEE standard; (a) V_w = 0.56 m/s, (b) V_w = 1.12 m/s, (c) V_w = 1.67 m/s, and (d) V_w = 2.22 m/s

To sum up, in practical applications, the improved EHT model calculates ampacity by selecting the temperature of any point on the surface of the Al ball. Compared with the IEEE standard, the maximum error is no more than 6%, which can meet the requirements of actual engineering applications. It shows that the improved EHT model calculation results are reliable and can meet the safe operation requirements of the power system in practical engineering applications.

Sensitivity analysis of the improved equivalent heat transfer model

Sensitivity calculation

According to the ampacity calculation process of the improved ETH model, the input parameters of the model include the Al ball temperature, T_s, the ambient temperature, T_a, the solar irradiance, Q_s, and the wind direction, φ. In practical applications, the deviations in the measurement of these parameters can result in inaccurate calculation of ampacity by the improved EHT model. As a result, the sensitivity analysis can be used to determine the degree of influence for this interference on the improved EHT model. The following analysis focuses on the sensitivities of the Al ball temperature, the ambient temperature, the solar irradiance, and the wind direction the ampacity results calculated by the improved ETH model.

The ampacity result calculated by the improved EHT model has a functional relationship I (T_s, T_a, Q_s, φ). Taking the sensitivity of the parameter x to the ampacity as an example,

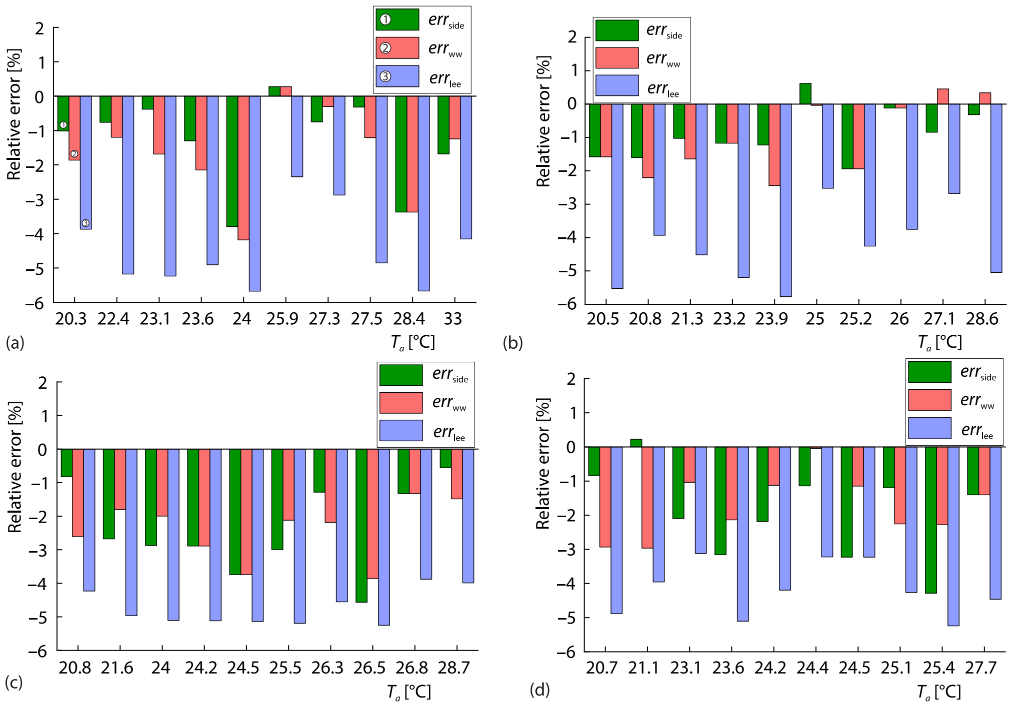

Figure 11. Relative errors of ampacity results from improved EHT model and IEEE standard; (a) V_w = 0.56 m/s, (b) V_w = 1.12 m/s, (c) V_w = 1.67 m/s, and (d) V_w = 2.22 m/s

the partial derivative of the parameter x to the ampacity needs to be solved to calculate the sensitivity. The calculation for the sensitivity of ampacity relative to the parameter x is shown:

$$S_x^I = \frac{\partial I}{\partial x}\frac{x}{I} = \frac{\dfrac{\partial I}{I}}{\dfrac{\partial x}{x}} \tag{15}$$

Bring T_s, T_a, Q_s, φ into x, respectively to get the sensitivity of ampacity relative to these parameters. According to the improved EHT model and eq. (15), the ampacity and sensitivity are calculated. In the calculation process, the parameters values and ranges are shown in tab. 1.

Table 1. Value range of parameters in sensitivity calculation

Sensitivity	T_s [°C]	T_a [°C]	Qs [Wm^{-2}]	φ [°]
I relative to T_s	38-70	35	0	90
I relative to T_a	45	0-40	0	90
I relative to Q_s	40	35	0-1000	90
I relative to φ	40	35	0	0-90

The ampacity and sensitivity are represented by I_{amp} and S_I, respectively, and the analysis results are shown in fig. 12.

In figs. 12(c) and 12(d), the sensitivity of solar irradiance and wind direction current carrying capacity is about 0, and the change of current ampacity is relatively small. This shows that the solar irradiance and the wind direction are weak correlation parameters of the improved EHT model. When there is a measuring error in the solar irradiance and the wind direction, the influence on the model is small. Therefore, the influence of the disturbance from solar irradiance and wind direction on the model are no longer discussed in this paper. In figs. 12(a) and 12(b), the ampacity is more sensitive to the Al ball temperature and the ambient temperature, especially for the Al ball temperature. When the Al ball temperature is low, the sensitivity is high. When the temperature of the Al ball changes by 1%, the ampacity calculated by the model changes by more than 6%. The ampacity changes dramatically as the Al ball temperature changes. Therefore, the Al ball temperature is a strong correlation parameter of the improved EHT model. The improved EHT model is greatly affected by the temperature disturbance of the Al ball. Based on the aforementioned analysis, it is necessary to determine the application scope of the improved EHT model.

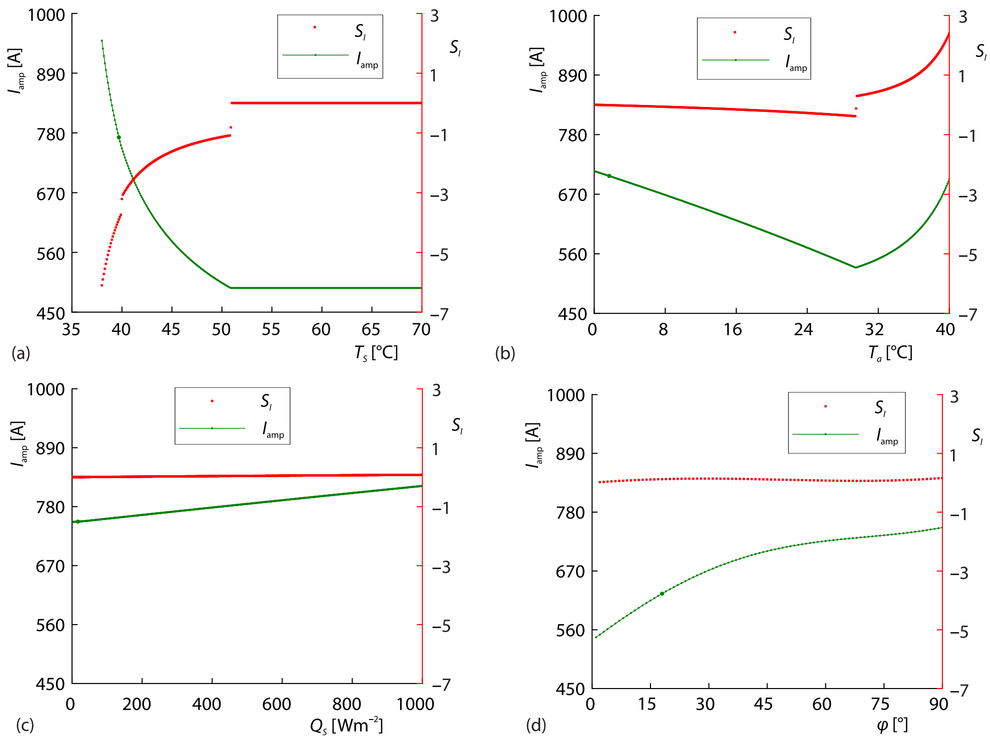

Figure 12. Sensitivity analysis of improved EHT model; (a) Al ball temperature, (b) ambient temperature, (c) solar irradiance, and (d) wind direction

Reliability critical conditions

In order to evaluate the reliability of the improved EHT model in practical application, the application scope of the improved EHT model is determined. In this paper, the sensitivity of calculated ampacity relative to the Al ball temperature is controlled within –3 to +3. According to this restricted condition, the range of model parameters is determined.

It can be seen from fig. 12(a) that the absolute value of the ampacity sensitivity relative to the Al ball temperature decreases with the increase of the Al ball temperature. When the Al ball temperature exceeds the critical value $T_{\mathrm{s,lim}}$, the sensitivity can be limited within ±3.

Therefore, the critical Al ball temperature needs to be determined to evaluate the reliability of the model. The temperature range of the Al ball is changed under different ambient temperatures. When the heat source power of the Al ball is constant, the determined critical Al ball temperature is a function related to the ambient temperature.

According to the improved EHT model and the designed MATLAB program, the related function between the critical Al ball temperature and the ambient temperature is determined. The ambient temperature is 0-40 °C, and under each ambient temperature value, the Al ball temperature is higher than the ambient temperature but not more than 70 °C. Then, a series of sensitivity values can be obtained. When the sensitivity is within ±3, the Al ball temperature is the critical value at this ambient temperature. Using this method, a set of Al ball critical temperature $T_{\mathrm{s,lim}}$ and ambient temperature T_{a} data are obtained. The curve fitting is performed on the obtained data to get the correlation between the critical Al ball temperature and the ambient temper ature:

$$T_{\mathrm{s,lim}} = 1.146 T_{\mathrm{a}} + 0.5341 \tag{16}$$

The residual analysis of the fitting results shows that R^2 is equal to 0.9994. This result indicates that it has good fitting and high reliability.

In summary, the reliability of the improved EHT model can be evaluated according to the correlation between the critical Al ball temperature and the ambient temperature. In practical applications, if the measured Al ball temperature is lower than the critical Al ball temperature, it indicates that the reliability of the model is low, and the influence of the disturbance caused by the measuring error cannot be ignored. Moreover, the Al ball temperature can be higher than the critical temperature by adjusting the heat source power of the Al ball in the EHT equipment to meet the reliability requirements of the model.

Conclusions

At first, the EHT model proposed in [17] is improved in this paper. The improvement includes two aspects. One is that the effect of air density and air dynamic viscosity are considered when establishing the correlation between the conductor and the Al ball. The other is that the experimental correlation parameters of the Al ball are determined again according to the theoretical calculation formula of convection heat transfer. Subsequently, combined with the experimental platform, the operation of the Al ball in the EHT equipment is simulated, and the improved EHT model is verified by IEEE standard. Finally, the sensitivity of the improved EHT model is analyzed, and the critical conditions of the model reliability are determined.

The results show that the improved EHT model has greatly improved the result accuracy in application, and the improvement effect is significant. Moreover, compared with the original EHT model, the improved EHT model can choose the steady-state temperature at any position on the surface of the Al ball to calculate the conductor ampacity, and the relative error does not exceed 6%. Based on the sensitivity analysis results, the Al ball temperature is a strong correlation parameter of the improved EHT model. The improved EHT model is reliable, which can meet the safe operation requirements of the power system in practical engineering applications.

Acknowledgment

This research was funded by the Science and Technology Project of China Southern Power Grid, grant number GDKJXM20185588.

Nomenclature

IEEE – Institute of Electrical and Electronic Engineers
EHT – equivalent heat transfer
DTR – dynamic thermal rating
STR – static thermal rating

References

[1] Mbuli, N., *et al*., A Literature Review on Capacity Uprate of Transmission-lines: 2008 to 2018, *Electric Power Systems Research*, *170* (2019), May, pp. 215-221
[2] Teh, J., *et al.*, Prospects of Using the Dynamic Thermal Rating System for Reliable Electrical Networks: A Review, *IEEE Access*, *6* (2018), Apr., pp. 26765-26778
[3] Uski, S., Estimation Method for Dynamic Line Rating Potential and Economic Benefits, *International Journal of Electrical Power & Energy Systems*, *65* (2015), Feb., pp. 76-82
[4] Silva, A. A. P., Bezerra, J. M. B., Applicability and Limitations of Ampacity Models for HTLS Conductors, *Electric Power Systems Research*, *93* (2012), Dec., pp. 61-66
[5] Thirumurugaveerakumar, S., *et al*., Prediction and Comparison of Size of the Copper and Aluminum Bus Duct System Based on Ampacity and Temperature Variations Using Matlab, *Thermal Science*, *22* (2018), 2, pp. 1049-1057
[6] House, K. E., Tuttle, P. D., Current-Carrying Capacity of Acsr, *Electrical Engineering*, *77* (1958), 8, pp. 719-719
[7] Howington, B. S., Ramon, G. J., Dynamic Thermal Line Rating Summary and Status of the State-of-the-Art Technology, *IEEE Transactions on Power Delivery, PWRD*, *2* (1987), 3, pp. 851-858
[8] Kanalik, M., *et al*., Temperature Calculation of Overhead Power Line Conductors Based on CIGRE Technical Brochure 601 in Slovakia, *Electrical Engineering*, *101* (2019), 16, pp. 921-933
[9] Ľubomir, B., *et al*., Calculation of the Overhead Transmission-Line Conductor Temperature in Real Operating Conditions, *Electrical Engineering*, *103* (2021), 2, pp. 769-780
[10] Hasan, M. K., *et al*., An Improved Dynamic Thermal Current Rating Model for PMU-Based Wide Area Measurement Framework for Reliability Analysis Utilizing Sensor Cloud System, *IEEE Access*, *9* (2021), Jan., pp. 14446-14458
[11] Castro, P., *et al*., Study of Different Mathematical Approaches in Determining the Dynamic Rating of Overhead Power Lines and A Comparison with Real Time Monitoring Data, *Applied Thermal Engineering*, *111* (2017), Jan., pp. 95-102
[12] Foss, S. D., Maraio, R. A., Dynamic Line Rating in the Operating Environment, *IEEE Transactions on Power Delivery*, *5* (1990), 2, pp. 1095-1105
[13] Smolleck, H. A., Sims, J. P., Guidelines for the Selection and Operation of Bare ACSR Conductors with Regard to Current-Carrying Capacity, *Electric Power Systems Research*, *5* (1982), 3, pp. 179-190
[14] Seppa, T. O., Accurate Ampacity Determination: Temperature-Sag Model for Operational Real Time Ratings, *IEEE Transactions on Power Delivery*, *10* (1995), 3, pp. 1460-1470
[15] Bose, A., Smart Transmission Grid Applications and Their Supporting Infrastructure, *IEEE Transactions on Smart Grid*, *1* (2010), 1, pp. 11-19
[16] Polevoy, A., Impact of Data Errors on Sag Calculation Accuracy for Overhead Transmission-Line, *IEEE Transactions on Power Delivery*, *29* (2014), 5, pp. 2040-2045
[17] Liu, Z., *et al*., An Equivalent Heat Transfer Model Instead of Wind Speed Measuring for Dynamic Thermal Rating of Transmission-Lines, *Energies*, *13* (2020), 18, pp. 1-18
[18] ***, IEEE 738-2012, IEEE Standard for Calculating the Current-Temperature Relationship of Bare Overhead Conductors, in: IEEE Standard Association, Washington, USA, 2013, pp. 1-72
[19] Whitaker, S., Forced Convection Heat Transfer Correlations for Flow in Pipes, Past Flat Plates, Single Cylinders, Single Spheres, and for Flow in Packed Beds and Tube Bundles, *AIChE Journal*, 18 (1972), 2, pp. 361-371
[20] Hsissou, R., *et al.*, Polymer Composite Materials: A Comprehensive Review*, Composite Structures*, *262* (2021), Apr., pp. 1-15
[21] Hua, G. W., *et al*., Research on Identification of Model Predictive Control Parameters for Interline Power Flow Controller, *GuangDong Electric Power*, *34* (2021), 2, pp. 19-27
[22] Liu, K., *et al*., Study on Value of Wind Load Adjustment Coefficient for Foundation Design of Tangent Tower of Transmission-line, *GuangDong Electric Power*, *32* (2019), 8, pp. 141-149

Paper submitted: June 11, 2021
Paper revised: October 11, 2021
Paper accepted: November 8, 2021